JVSTB
JOURNAL OF VACUUM SCIENCE AND TECHNOLOGY B

X-ray and electron-beam lithography of three-dimensional array structures for photonics

F. Romanato, D. Cojoc, E. Di Fabrizio, M. Galli, and D. Bajoni

Citation: J. Vac. Sci. Technol. B **21**, 2912 (2003); doi: 10.1116/1.1629295
View online: http://dx.doi.org/10.1116/1.1629295
View Table of Contents: http://avspublications.org/resource/1/JVTBD9/v21/i6
Published by the AVS: Science & Technology of Materials, Interfaces, and Processing

X-ray and electron-beam lithography of three-dimensional array structures for photonics

F. Romanato,[a] D. Cojoc, and E. Di Fabrizio
TASC-INFM, S.S. 14, Km 163.5 34012 Basovizza, Trieste, Italy

M. Galli and D. Bajoni
INFM and Dip. di Fisica "A. Volta," Università di Pavia, Via Bassi 6, I-27100 Pavia, Italy

(Received 3 September 2003; accepted 6 October 2003; published 9 December 2003)

The possibility to realize three-dimensional (3D) photonic crystals and the capability to internally insert a waveguide path poses a big challenge from the fabrication point of view. We present a fabrication method for a 3D lattice with designed linear defects by multitilt x-ray exposures and electron-beam lithography. This combination of different lithographies has been developed to control the design and the realization of the linear defects inside the three-dimensional structure. This method has been applied for the fabrication of Nickel Yablonovite lattices with a lattice parameter of 1.8 μm and a total thickness of 15 μm, a value that allows us to achieve a full three-dimensional optical behavior as confirmed by variable angle reflectance measurements. [DOI: 10.1116/1.1629295]

I. INTRODUCTION

Molding the flow of light represents one of the goals of photonics. Computational experiments showed that a full waveguide control can be obtained by allowing light to travel along linear defects designed in three-dimensional (3D) photonic crystals (PCs),[1–3] i.e., dielectric arrays with lattice parameters comparable with the wave light. The possibility to realize a 3D PC for the visible spectrum and, moreover, a waveguide defect (WGD) in the lattice structure represents a considerable challenge from the fabrication point of view. This purpose requires a technique that is able to generate large and cheap 3D structuring and, at the same time, that can introduce a designed photonic network inside the 3D lattice.

At the very beginning of the research on 3D PCs, an original fabrication method was proposed by Yablonovitch[4] using millimeter-scale periodic arrays of holes drilled in a dielectric material to realize a 3D PC at microwave frequencies. The resulting lattice structure showed a net energy band gap and took his name: Yablonovite. Hole drilling was also implemented using tilted x-ray lithography (XRL) for the fabrication of a PC with a lattice parameter in the range of hundreds of microns,[5] and subsequently, in the range of 1 μm by Cuisin *et al.*[6]

Differently by other parallel approaches,[7–10] in XRL it is possible to introduce all the information about the lattice structure in the form of pattern on the x-ray mask. We are not referring only to the obvious characteristics (symmetry, lattice parameter, filling factor, etc.), but also to the possibility of extended defects generation by an appropriately designed of mask pattern. We present our progress for the fabrication of a WGD inside 3D period arrays by means of tilted XRL also in combination with electron-beam lithography (EBL). This fabrication method has been applied to metallic 3D PCs, which are advantageous in high frequency region (greater than 100 THz) owing to the fact that metals become almost completely reflectors. The metallic structure can also be envisaged as a template to be filled with semiconductor material to realize metallodieletric PCs, or after the removal of the metal, as a pure dielectric PC. Looking forward to this kind of application, we specifically fabricated a nickel Yablonovite structure with lattice parameter of 1.8 μm, interesting for photonic application at a similar light wavelength. First-hand optical reflectance measurements had shown that these metallic structures have characteristic resonances as required for 3D PCs. In particular, we addressed the issue concerning the optimization of the 3D structure thickness. This is an important parameter, because it determines the number of lattice planes parallel to the sacrificial substrate that must be large enough to ensure a bulk-like optical behavior.

II. EXPERIMENTS

Proximity x-ray lithography was performed at the LILIT beamline[11] located at Elettra Synchrotron (Trieste, Italy).[12] The LILIT beamline was designed for performing both soft and hard x-ray lithography, allowing the possibility to choose the required energy window from the quite wide energy spectrum provided by Elettra bending magnets (from a few hundred eV to 25 keV). In the present work, a *medium* hard spectrum was selected (from 500 eV to 4 keV) in order to facilitate the exposure of thicker resist ($>$15 μm). Several x-ray masks were used for this experiment. These masks consist of a gold film, which is typically 350 nm thick, patterned in a triangular array of circular holes supported on a self-standing 1-μm-thick Si_3N_4 membrane.

A tilted sample holder was fabricated having a the tilt angle of θ=35.26° in order to correctly generate Yablonovite lattices from triangular mask arrays. The tilted mask and the sample were mounted together on the mask stage of the

[a]Electronic mail: romanato@tasc.infm.it

x-ray stepper, ensuring a permanent and fixed contact between mask and sample. By using markers and references it was possible to align the fixed system mask+sample to the x-ray beam. The sample holder is capable of performing circular movements, thereby enabling a complete azimuth rotation with a step size of 15°. No relative alignment mask to sample could be performed on the tilted sample holder.

A gold metalization (5 nm thick) was deposited on silicon substrates, and subsequently, they were spun with polymethyl methacrylate (PMMA) resist of different thicknesses (from 10 to 20 μm). PMMA was developed for 1 min in 1:1 solution of methyl Isobutyl ketone and isopropil alcohol (MIBK:IPA) and rinsed in IPA. The patterned areas were first filled by electroplating deposition with nickel, and then PMMA was stripped in acetone at 50 °C.

Electron-beam lithography with a JEOL 6400 at 30 keV was performed for the generation of the mask pattern. A 450-nm-thick SAL negative resist was exposed and cured with a prebaking at 105° for 60 s and postbaking at 105° for 75 s, and finally, developed in MF312 diluted 1:1 in H_2O. EBL was also performed for the generation of the WGD as described in the following.

Optical characterization was performed by means of the variable angle reflectance technique introduced by Astratov.[13] The reflectance was measured in the 0.3–1.5 eV spectral range by means of a Fourier transform spectrometer (Bruker IFS-66) at a spectral resolution of 1 meV. Light from a broadband Hg arc lamp was collimated and focused down to a spot of about 100 μm on the sample surface with a spread angle of $\pm 1°$. The angle of incidence was varied between 5.4° and 59.4° with steps of 5.4° in the plane of incidence normal to the sample surface (classic mount). Measurements were performed for light incident along the high symmetry orientation Γ-X of the sample, both for transverse electric (TE) and transverse magnetic (TM) polarized light.

III. RESULTS AND DISCUSSION

A. Generation of 3D structures

The idea underlying the realization of a three-dimensional lattice by x-ray lithography is quite simple. Let us consider the pattern of an x-ray mask exposed on the resist sample at different directions. This can be achieved by tilting the mask +sample set in front of the x-ray beam.[14] From the frame of reference of the sample, each opening of the x-ray mask can be considered as a collimated light source that expose the resist along designated directions, generating different holes.

A single hole generates a tetrahedral tripod-like structure (Fig. 1 inset, structure A). When the x-mask openings are close enough, the light paths superpose and the holes intersect (Fig. 1 inset, structure B; 15 pillars are generated by five close holes of the x-mask). When the x-ray mask openings were organized in plane array and the exposure directions are along the major axis of the associate 3D lattice structure, then the exposed pillars organize themselves in a 3D lattice. Specifically, if the planar array has triangular geometry and three exposures take place every 120° rotation, the lattice that is generated is the Yablonovite (Fig. 1). At LILIT beamline, samples as large as 2000 mm^2 can be expose at once and a step-and-repeat process allows us to cover complete 5 in. wafers.

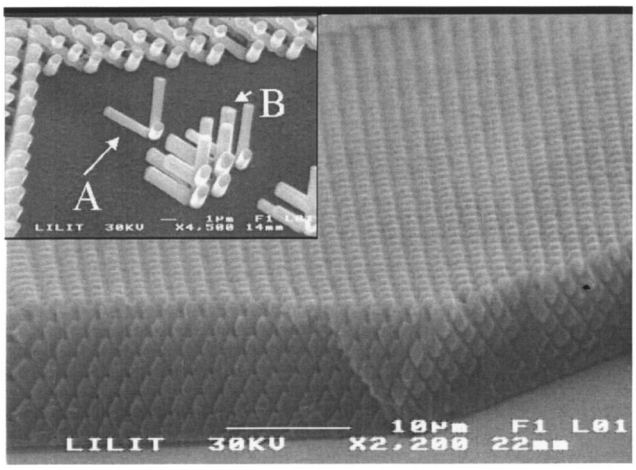

FIG. 1. Yablonovite lattice generated by x-ray lithography on a PMMA film. Inset: crossing pillars made by nickel and fabricated by multiexposure tilted x-ray lithography. (A) Tripod-like structure generate by a single hole in the x-ray mask. (B) Five crossing tripods generated by five close holes.

B. Thickness optimization

Looking forward to device application, not only the lateral dimension but also the 3D PC thickness plays an important role: it must be large enough to provide full 3D optical behavior. In the literature several different critical thicknesses have been reported depending on the specific structure and material taken into account. Fleming *et al.*[15] have shown that for metallic structures four plane lattices parallel to the substrate are enough to completely open the band gap. This number is certainly too low for semiconductor PCs. The rule of thumb that the thickness must be much larger than the wavelength (i.e., of the lattice parameter) implies that the number of lattice planes must be greater at the list than 5–7. Moreover, in the perspective of the introduction of a WGD in the middle of the lattice structure, the critical number of lattice planes, N_c, doubles, as required above and below the WGD.

From a lithographic point of view, a constrain on N_c becomes a condition on the length of the metallic pillars. In the case of Yablonovite, the pillar length along the tilted directions is $L = N_c a$, i.e., proportional to lattice parameter a. For a between 1 and 2 μm, this means that L would range between 10 and 28 μm. Because, typically, the pillar diameter, d, ranges between $a/3$ and $a/2$, conditions on L mean that the aspect ratio of the pillars, $AR = L/d$, must be of the order of $2N_c - 3N_c$, i.e., between 23 and 42 μm. These are aspect ratios that XRL can accomplish also during tilted exposures. An example of tilted pillars, nickel made, is shown in Fig. 2. Their length and diameter (at the surface) are, respectively, 25 and 0.55 μm for a resulting aspect ratio of 45.

However, new lithographic problems arise using tilted exposures. One is a progressive thinning of the pillars as function of the thickness. A closer view of Fig. 2 shows that the

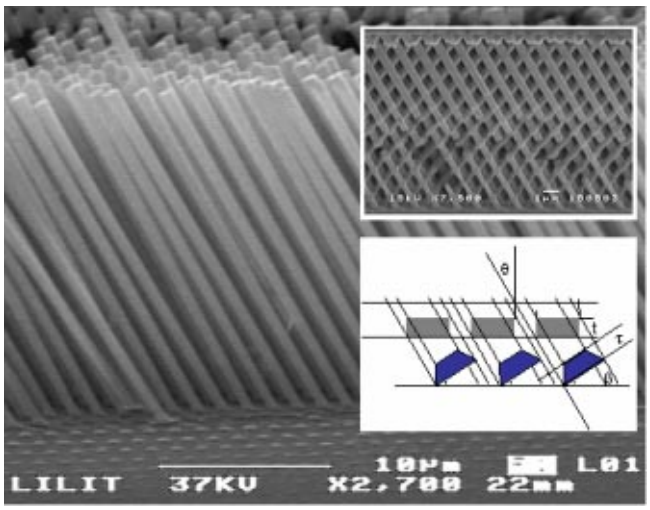

FIG. 2. Single x-ray exposure of tilted pillars with aspect ratio of 45. Bottom inset: geometry of tiled exposures. The absorber digital profile transforms into a trapezoidal-like profile. Top inset: Yablonovite lattice of crossing pillars generates up to 14 parallel lattice planes.

pillars at the bottom are 145 nm thinner than on the top. Typical values of thinning measured on other samples are of the same order of magnitude, i.e., a diameter reduction of 0.6% per unit length, an amount that cannot be accepted in the design of a PC.

The origin of the vertical thinning is addressed to tilted exposures. Typically, in a perpendicular exposure the mask pattern is shadowed on the resist by the absorption of the x rays. In this case, the vertical edges of the gold mask profile do not determine any distortion of the pattern (neglecting, in a first approximation, diffraction effects). On the contrary, in tilted exposures a fraction of the x-ray beam impinges on the lateral walls of the mask determining a length path through the absorber that is proportional to the position height on the lateral wall (bottom inset of Fig. 2). It results in the box-like profile of the x-ray mask pattern being transformed into an apparent trapezoidal-like profile (TLP). The vertical wall edge broadening amounts to $\beta = t\tan(\theta)$, where t is the thickness of the gold mask absorber and θ is the tilting angle. As a consequence, also the exposed dose profile suffers a broadening resulting from modulation of the TLP with the gold absorption coefficient.

The vertical thinning can be explained as follows: at the beginning, the developing front starts to open on the resist surface holes in correspondence of the exposed areas and, successively, proceeds along the exposed direction. However, due to the TLP, the developing front in the open region progressively enlarges the hole size. The holes of the top regions exploiting a longer developing time open wider with respect to the deeper regions that are reached by the developing front only successively.

The solution for this problem is obtained by developing over time of the order of 50% with respect of the time required for the developing front to reach the substrate interface. Developing over time provides a full development for the bottom regions, in the meantime the top regions have already reached their maximum size. This method provides an almost complete straightening of the pillars with a residual thinning effect that, typically, is smaller than 3×10^{-4}, i.e., the diameter size reduces 3×10^{-4} μm for each micron along the pillar length.

However, developing over time can be performed without causing structural crashes of the patterned areas only if the mask contrast is sufficiently great, i.e., if the thickness of the gold absorber is sufficiently thick. On the other hand, a thick mask increases the broadening of the TLP. The mask thickness becomes therefore a crucial parameter that must be accurately optimized case by case.[16]

Typically, in order to successfully expose 20 μm of PMMA resist it is necessary that a mask contrast at the list of 0.8, i.e., a mask thickness of 330 nm.[17] During a tilted exposure a positive contribution to the mask contrast is provided by the apparent absorber thickness that increases as $\tau = t/\cos(\theta)$. On the other hand, a negative contribution is due to multiple exposures. In order to deliver the necessary radiation dose for each tilt of the three directions, the opaque regions of the x-ray mask must absorb a triple radiation dose. The two contributes have a partial compensation and a final contrast of 0.8 for triple tiled exposure is achieved with a theoretical increasing to 360 nm of the mask thickness.[18] As a confirmation of this estimation, the top inset of Fig. 2 (Ref. 19) shows a successful exposure of a Yablonovite 3D structure that has been generated from a x-ray mask patterned with a triangular array of 1.3 μm lattice parameter and 345 nm absorber thickness. The 3D lattice of crossing pillars generates up to 14 parallel lattice plane. The developing over time in this case was estimated to be 33% (90+30 s overtime) and it was enough to almost completely straighten the pillars, leaving only a residual vertical thinning of 1×10^{-3}.

C. Optical characterization

Preliminary optical characterizations performed on the sample shown in Fig. 2 are reported in Fig. 3. The experimental reflectance spectra show several sharp features which display a well-defined dispersion in their energy position as the angle of incidence is varied, both for TE and TM polarizations. These kinds of resonances, which are very similar to those observed in two-dimensional (2D) and 3D dielectric photonic crystals,[20,21] are likely to be associated with the excitation of the 3D photonic bands of the metallic sample. The observation of such structures is a clear indication of the very good quality and true three-dimensionality of the samples. In particular, the sharp minimum observed at low energy in the TM reflectance spectra may be related to the excitation of a surface-plasmon polariton, while the other step-like features are most probably associated with the excitation of the allowed photonic modes of the metallic 3D structure. The determination of the photonic band dispersion may be extracted from the energy positions of the structures observed in the reflectance curves versus the wave vector $k = (\omega/c)\sin\theta$ of the incoming radiation field. However, the unambiguous interpretation of the experimental spectra

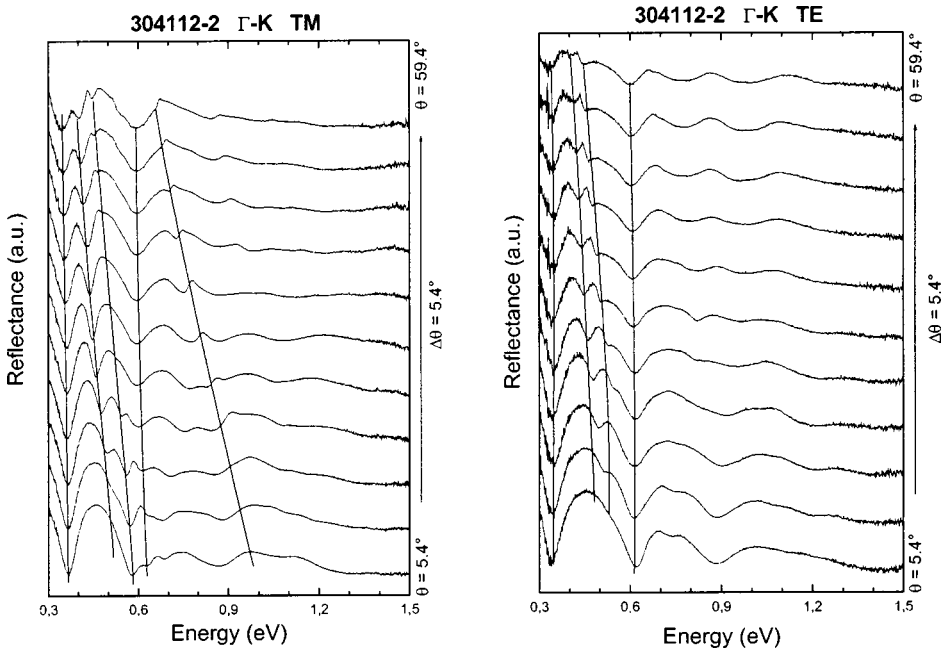

FIG. 3. Variable angle reflectance of the sample shown in Fig. 2 for light incident along the $\Gamma - K$ orientation, for TE and TM polarizations. The angle of incidence is varied from 5.4° to 59.4° with steps of 5.4°. The curves are vertically shifted for clarity.

would require the development of a theoretical model and the comparison of the experimental measurements to the calculated photonic bands.

D. Role of electron-beam lithography

There is still a residual drawback in the realization of multiple tilted exposures. The developing overtime provides a final over size of the pillars diameters with respect to the mask hole dimensions; the greater the TLP broadening, the greater is the overall size. In the case of the sample shown in Fig. 2 the original holes diameter in x-ray mask were 445 nm (by design was selected $d = a/3 = 433\,\text{nm}$) against a maximum pillar diameter of 550 nm. This final value is in good agreement with the estimated value of the TLP, which amounts to 562 nm. The residual difference can be explained by the convolution of the TLP with the gold absorption coefficient that generated under exposed tails.

This effect can be computed and taken into account as a correction factor in the design and on the fabrication of the x-ray mask pattern. In fact, EBL allows almost complete freedom on the design and fabrication of the main parameters of x-ray mask pattern array (symmetry of the lattice, lattice parameter, and dot and shape size). EBL, furthermore, gives the possibility of designing selectively specific part of the x-ray mask in order to introduce defects or special pattering, i.e., missing dots, and dots with changed size or complex structure. As an example, we have previously considered structure A in Fig. 1 as a single isolated tripod-like structure. This structure represent, *per se* a simple lithographic exercise, but it is sufficient to take out a hole in the triangular array of mask pattern to generate exactly a negative tripod in Yablonovite structures. This type of defect will represent the unit structure for a device connecting three waveguide in 3D PC. Several types of defects can be envisaged that can be directly exposed on the resist and their geometry can be usefully exploited in order to generate complex structures. However, these types of defects are limited by their tilted or vertical direction with respect to the substrate interface. What is really interesting is the possibility of fabricating a WGD parallel to the substrate that can be introduced inside the PC structure.

It is useful to remember that the final aim is the generation of a defect in the template of the 3D structure that after the semiconductor infiltration and metallic etching will leave an empty tube. Therefore, in the template it must appear like a solid line. Our approach consists of the combined use of EBL and XRL (Fig. 4). Some lines are written with EBL on the surface of a PMMA film previously exposed with XRL. Afterwards, a second PMMA film is spun above the first one and a second x-ray exposure is performed. Finally, the whole PMMA multilayer has been developed at once. The basic idea is to introduce linear defects at the interface between the two PMMA layers and perform around it a 3D lattice by XRL (Fig. 5). An EBL dose matrix has been performed: several lines, 2 μm wide and longer than the total 3D lattice ($400\times400\ \mu\text{m}^2$) have been exposed at doses ranging from 50 to 110 $\mu\text{C/cm}^2$ in steps of 20 $\mu\text{C/cm}^2$ (Fig. 5). The results show that the exposed line defects at the interface between the top and bottom 3D lattice have been, indeed, gold filled after the development and the electrolytical growth. Details of the lines at different doses show that both vertical and lateral broadening has been achieved for the higher doses (right-bottom inset of Fig. 5). For the lowest dose a good vertical confinement but a residual lateral broadening still remains (left-bottom inset of Fig. 5).

Two crucial elements can allow us to realize these linear defects. The first is the low dose exploited for the EBL in order to develop only a thin interface line. The second is the connected structure of the 3D lattice that allows us to develop both the top and bottom PMMA layers and the line at

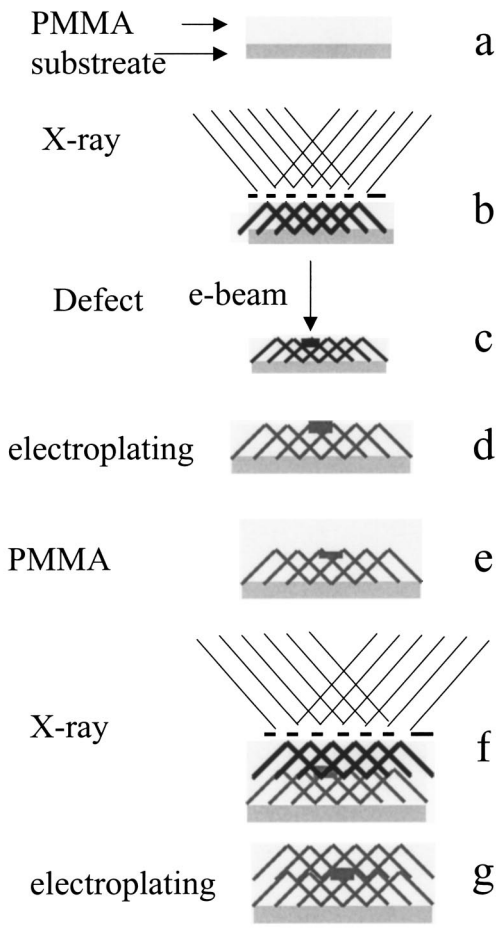

FIG. 4. Scheme of the process for the fabrication of waveguide defect in three-dimensional structures. (A) PMMA spun on a substrate, (b) multitilt x-ray exposure and development, (c) electron beam lithography of linear defect, (d) metal electroplating, (e) second PMMA spun, (f) second x-ray exposure and development, and (g) second metal electroplating and final (not shown) PMMA strpping.

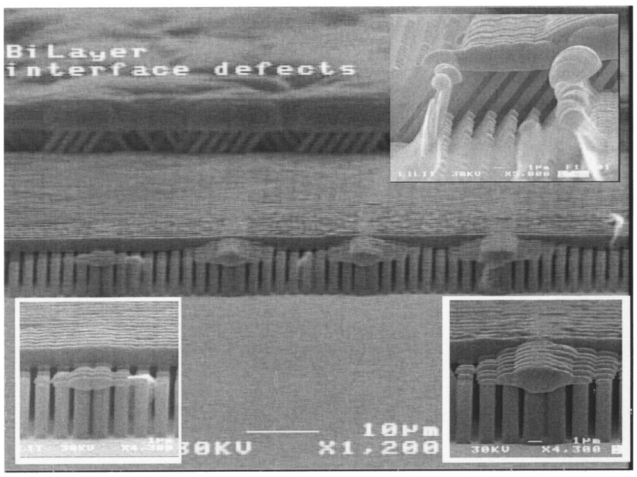

FIG. 5. Linear defect parallel to the substrate and inserted at the interface of two 3D lattices generated by electron beam lithography with different doses. Details of the lowest (left bottom inset), highest (right bottom inset) dose defect and of the top–bottom alignment (right top inset) are shown.

the interface while keeping the whole lattice standing.

The vertical alignment between the top and the bottom layer is a critical parameter. Only a few nanometers of tolerance, in principle, can be admitted to avoid pillar misalignments. This accuracy requires a specific system of alignment not available at the present. A rough mask+sample prealignment was performed under optical microscopy. By chance, a good alignment was obtained (top inset of Fig. 5) which confirms the validity of the process but requires the development of a specific system of alignment.

IV. CONCLUSION

The article reviews the present possibility to fabricate a 3D lattice structure by x-ray lithography for the fabrication of 3D metallic PC or as template for the infiltration of semiconductor. Discussion on the condition for tilted multiple x-ray exposure addressed, in particular, the optimization of an x-ray mask for a 1.8 μm lattice parameter Yablonovite structure that was realized with 550 nm pillar diameter, straightened within 1×10^{-3}, and with a length such that up to 14 parallel lattice planes have been achieved. Preliminary optical characterization showed resonance features, which are likely to be associated with the excitation of the 3D photonic bands of the metallic sample. Strategies for the introduction of controlled vertical and tilted linear defects to introduce in the x-ray mask design have been proposed. Preliminary results of an original combination of EBL–XRL for the introduction into 3D structure of parallel waveguide defects have shown the potentiality of the method proposed limited by the lack of a nanometric alignment system between the mask and the sample.

[1]J. D. Joannopoulos, R. D. Meade, and J. N. Winn, *Photonic Crystals* (Princeton University Press, Princeton, NJ, 1995).
[2]S. John, Phys. Rev. Lett. **58**, 2486 (1987).
[3]A. Chutinan, S. John, and O. Toader, Phys. Rev. Lett. **90**, 123901 (2003).
[4]E. Yablonovitch, Phys. Rev. Lett. **58**, 2059 (1987).
[5]G. Feiertag, W. Ehrfeld, H. Freimuth, H. Kolle, H. Lehr, M. Schmidt, M. M. Sigalas, C. M. Soukoulis, G. Kiriakidis, T. Pedersen, J. Kuhl, and W. Koenig, Appl. Phys. Lett. **71**, 1441 (1997).
[6]C. Cuisin, A. Chelnokov, J. M. Lourtioz, D. Decanini, and Y. Chen, J. Vac. Sci. Technol. B **18**, 3505 (2000).
[7]A. Imhof and D. J. Pine, Nature (London) **389**, 948 (1997).
[8]B. T. Holland, C. F. Blanford, and A. Stein, Science **281**, 538 (1998).
[9]A. M. Kapitonov, N. V. Gaponenko, V. N. Bogomolov, A. V. Prokofiev, S. M. Samoilovich, and S. V. Gaponenko, Phys. Status Solidi A **165**, 119 (1998).
[10]J. E. G. J. Wijnhoven and W. L. Vos, Science **281**, 802 (1998).
[11]F. Romanato, E. Di Fabrizio, I. Vaccari, M. Altissimo, D. Cojoc, L. Businaro, and S. Cabrini, Microelectron. Eng. **57**, 101 (2001).
[12]http://www.elettra.trieste.it/experiments/beamlines/lilit/index.html
[13]V. N. Astratov, D. M. Whittaker, I. S. Culshaw, R. M. Stevenson, M. S. Skolnick, T. F. Krauss, and R. M. De La Rue, Phys. Rev. B **60**, R16255 (1999).
[14]F. Romanato, L. Businaro, L. Vaccari, S. Cabrini, P. Candeloro, M. De Vittorio, A. Passaseo, M. T. Todaro, R. Cingolan, E. Cattaruzza, M. Galli, C. Andreani, and E. Di Fabrizio, Microelectron. Eng. **67-8**, 479 (2003).
[15]J. G. Fleming, S. Y. Lin, I. El-Kady, R. Biswas, and K. Ho, Nature (London) **417**, 52 (2002).
[16]Preliminar discussion on a general mask optimization process is discussed in Ref. 14.
[17]The mask contrast is defined as $c=D_{\mathrm{tr}}-D_{\mathrm{op}}/D_{\mathrm{opl}}$, where D_{tr} and D_{op} are, respectively, the dose exposed through the transparent and the opaque

areas of the mask. Because $D_{op}=D_{tr}\exp(-t/\mu_{Au})$, the contrast became $c=1-\exp(-t/\mu_{Au})$. The averaged gold absorption coefficient in the range of wavelength used is 0.21 μm.

[18]The contrast of x-ray mask used for the generation of a Yablonovite lattice is $c=[1-\exp(-t/\mu_{Au})]/(1+\exp(-t/\mu_{Au})]$.

[19]It must be notice that the picture has been obtained from a cross-section analysis of scratched PC and that visible pillars suffered the mechanical stress. This is the reason of some pillars failures.

[20]F. Romanato, L. Businaro, E. Di Fabrizio, M. Passaseo, M. De Vittorio, R. Cingolati, M. Patrini, M. Galli, D. Bajoni, L. C. Andreani, F. Giacometti, M. Gentili, D. Peyrade, and Y. Chen, Nanotechnology **13**, 644 (2002).

[21]M. Galli, M. Agio, L. C. Andreani, M. Belotti, G. Guizzetti, F. Marabelli, M. Patrini, P. Bettotti, L. Dal Negro, Z. Gaburro, L. Pavesi, A. Liu, and P. Bellutti, Phys. Rev. B **65**, 113111 (2002).